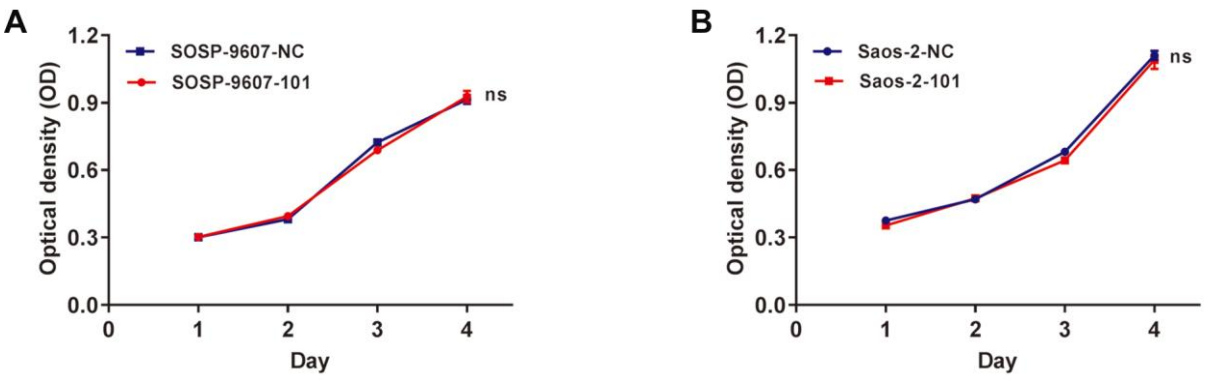

Figure S1. Effect of miR-101 on the proliferation of osteosarcoma cells observed via CCK-8 assay. (A) CCK-8 assay was performed on SOSP-9607-101 and SOSP-9607-NC cells. (B) CCK-8 assay was performed on Saos-2-101 and Saos-2-NC cells. Two-way ANOVA and Tukey's multiple comparisons test. ns, not significant (P >0.05).

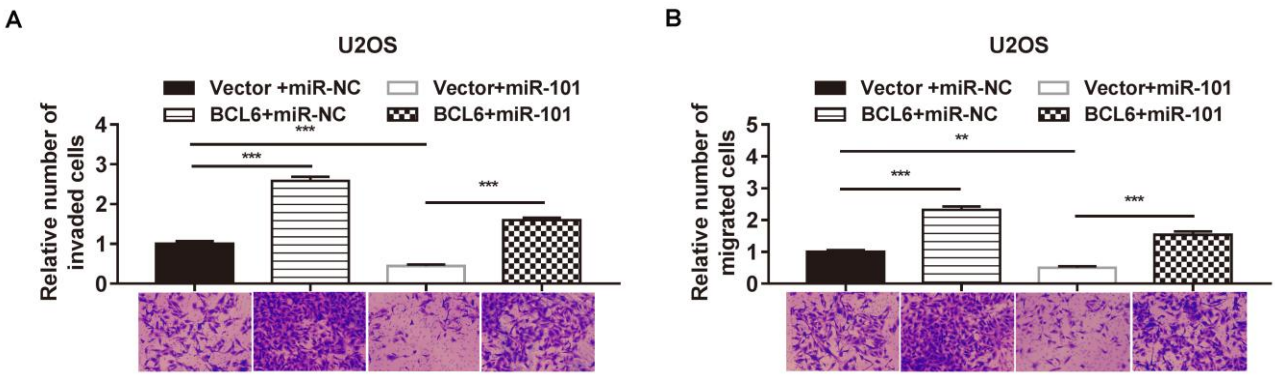

Figure S2. Effect of restoration of BCL6 expression on U2OS cell invasion and migration observed via Transwell assay. (A) Transwell invasion assay. (B) Transwell migration assay. One-way ANOVA and Tukey's multiple comparisons test. ** P <0.01; *** P <0.001.

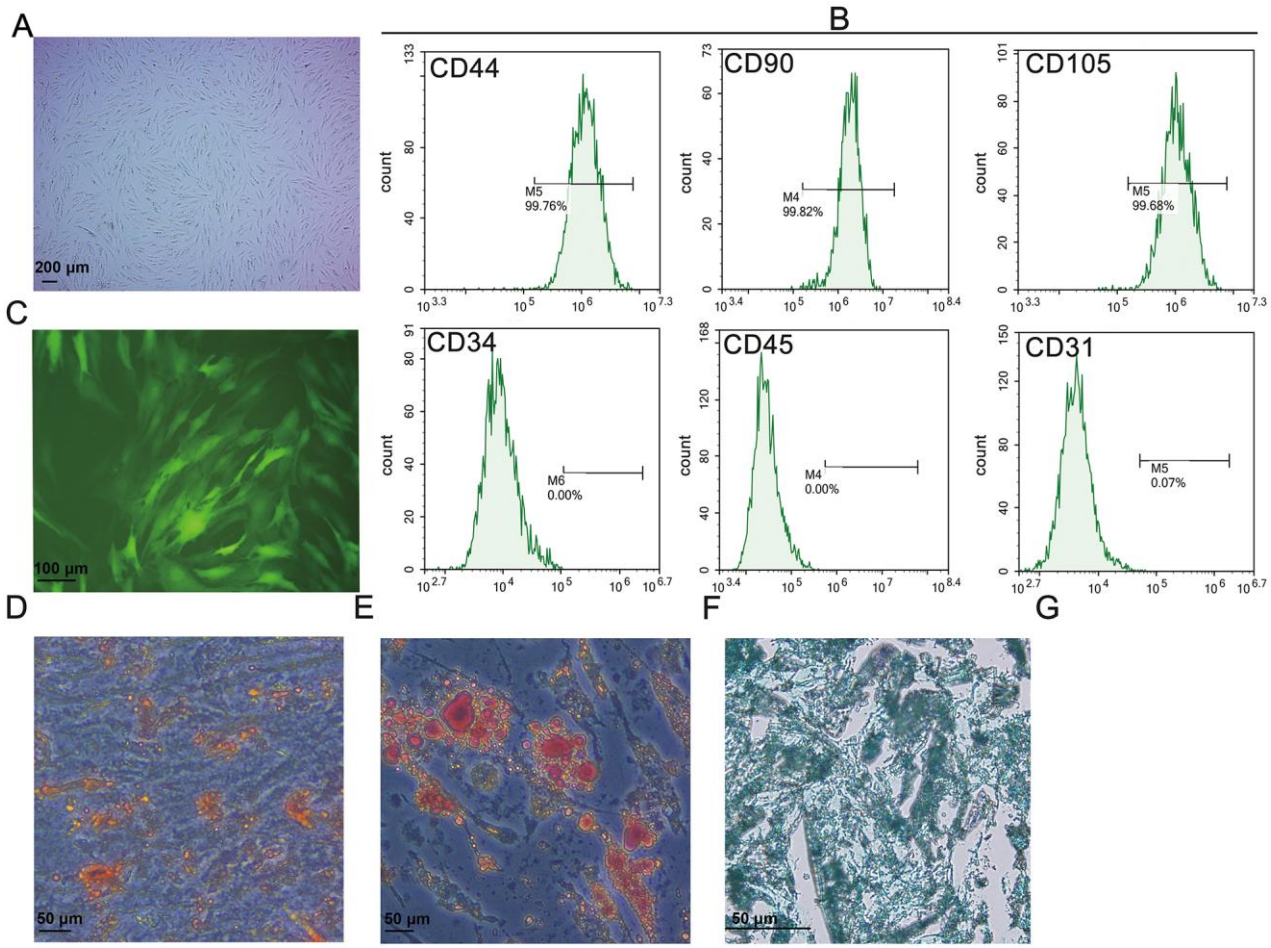

Figure S3. Identification of AD-MSCs and confirmation of the multi-lineage differentiation potential of engineered AD-MSCs. (A) Cellular morphology of AD-MSCs (passage 3) observed under light microscopy (40×). (B) Flow cytometric analysis of AD-MSC surface marker expression. (C) Successful lentiviral vector-mediated transduction of AD-MSCs confirmed by observation of GFP expression under fluorescence microscopy (100×). (D) Alizarin red S staining of engineered AD-MSCs after the induction of osteocyte differentiation (400×). (E) Oil red O staining of engineered AD-MSCs after the induction of adipocyte differentiation (400×). (F) Alcian blue staining of engineered AD-MSCs after the induction of chondrocyte differentiation (400×).

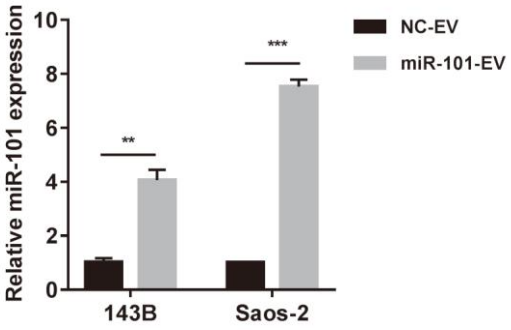

Figure S4. Detection of miR-101 expression in osteosarcoma cells, after uptake of AD-MSC-101-EVs by 143B and Saos-2 cells. NC-EV, EVs derived from AD-MSC-NC cells; miR-101-EV, EVs derived from AD-MSC-101 cells. Student's *t*-test. ** P <0.01; *** P <0.001.

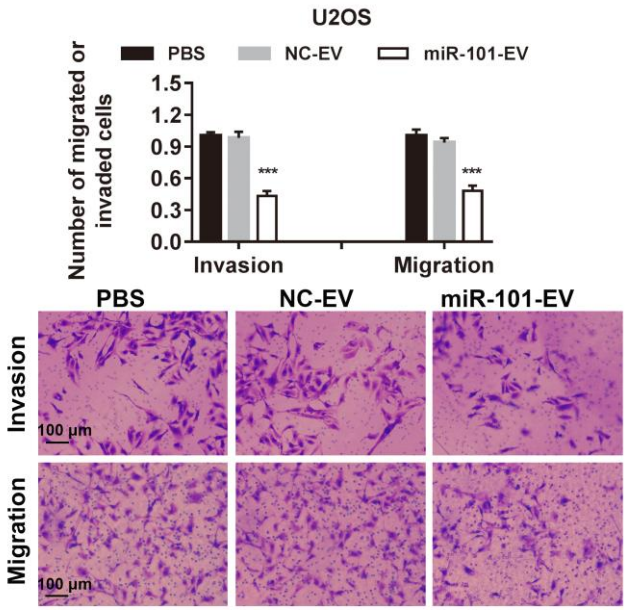

Figure S5. Effect of AD-MSC-101-EVs on invasion and migration abilities of U2OS cells observed via Transwell assay. NC-EV, EVs derived from AD-MSC-NC cells; miR-101-EV, EVs derived from AD-MSC-101 cells. One-way ANOVA and Tukey's multiple comparisons test. *** P <0.001 in comparison with PBS or NC-EV.

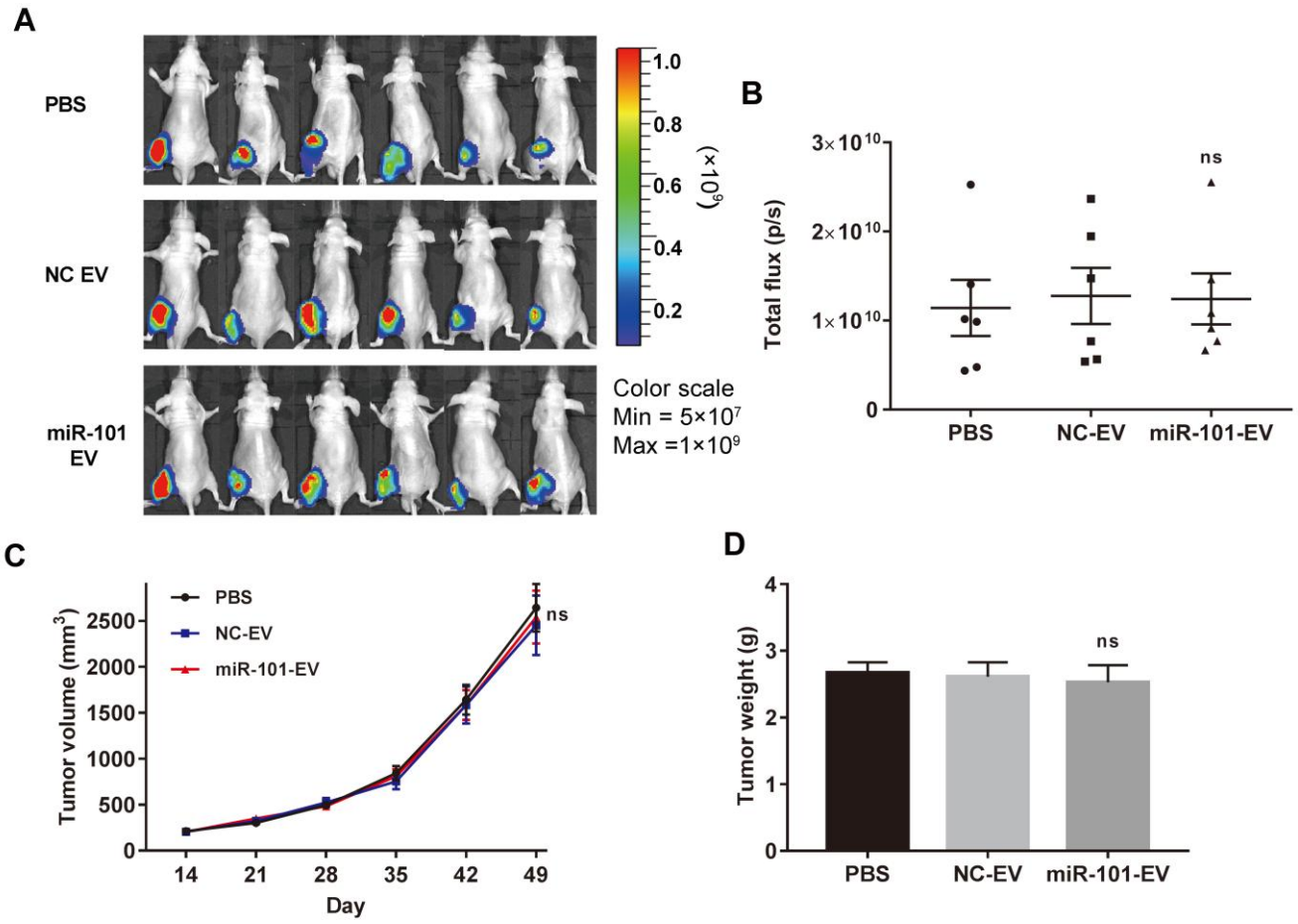

Figure S6. AD-MSC-101-EVs had little effect on the proliferation of osteosarcoma cells in vivo. NC-EV, EVs derived from AD-MSC-NC cells; miR-101-EV, EVs derived from AD-MSC-101 cells. (A) Primary tumors in the three groups were evaluated by IVIS at 7 weeks after tumor cell injection (n=6 per group). (B) Quantification of bioluminescence imaging. p/s: photons per second. Kruskal-Wallis test and Dunn's multiple comparisons test. (C) Proliferation curve for primary tumors. Volume = ½ × Length × Width^2. Two-way ANOVA and Tukey's multiple comparisons test. (D) Illustration of lung weight from the nude mice. One-way ANOVA and Tukey's multiple comparisons test. ns, not significant (P >0.05) in comparison with PBS or NC-EV.

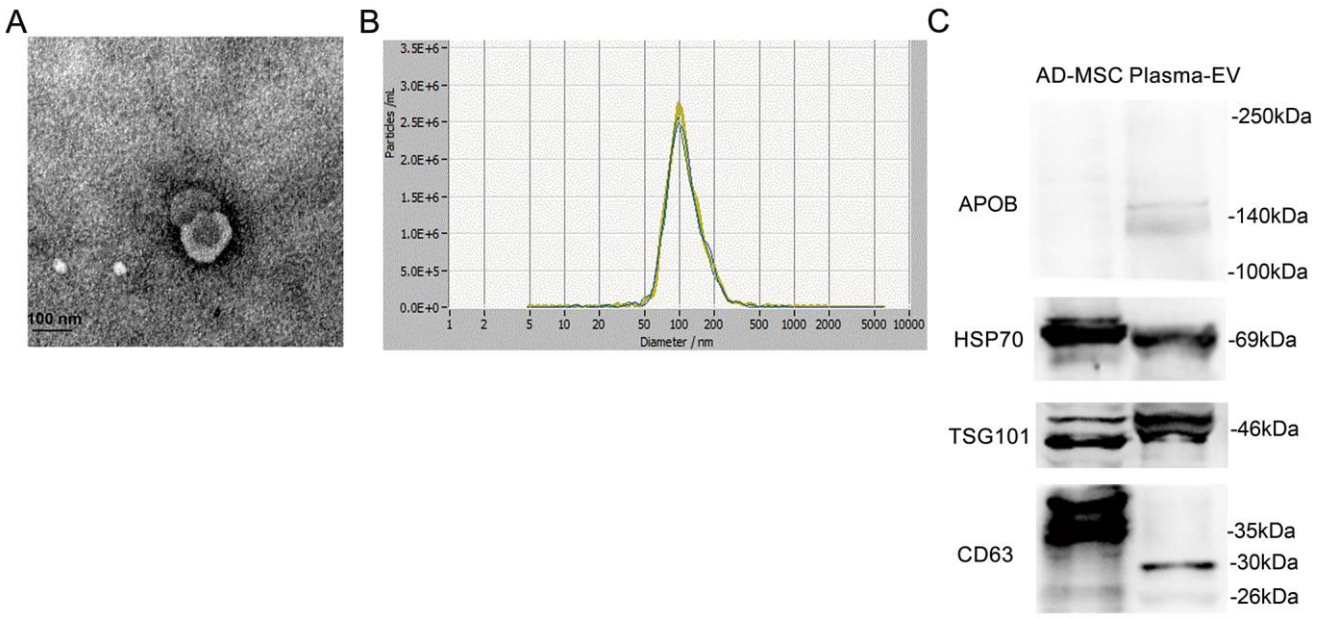

Figure S7. Characterization of plasma EVs. AD-MSC, adipose tissue-derived mesenchymal stromal cells; Plasma-EV, EVs derived from plasma. (A) Representative TEM of plasma EVs. (B) Results of NTA for plasma EVs (n=3). (C) Detection of surface markers of EVs was performed by western blotting. Briefly, 2 μg protein samples were loaded in each lane, and AD-MSC lysate was used as a control for EV characterization.

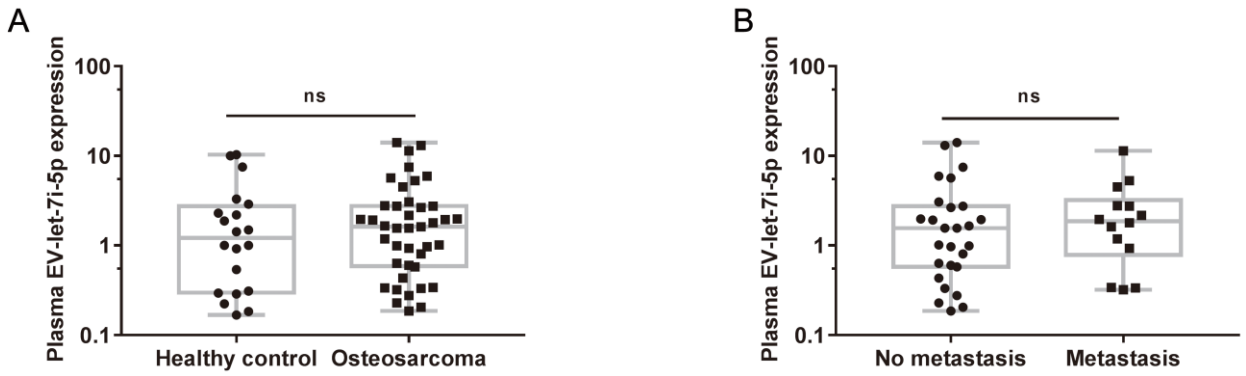

Figure S8. Plasma EV-let-7i-5p level was detected in healthy controls and osteosarcoma patients. (A) No significant difference in EV-let-7i-5p expression was observed between osteosarcoma patients and healthy controls. Mann-Whitney test. Error bars show minimum to maximum values. (B) No significant difference in EV-let-7i-5p expression was observed between osteosarcoma patients with metastasis and those without metastasis. Mann-Whitney test. Error bars show minimum to maximum values. ns, not significant (P >0.05).

Table S1. Characteristics of healthy controls and osteosarcoma patients.

Characteristics	Healthy controls (n=20)	OS patients (n=41)
Gender		
Male	12	27
Female	8	14
Age (years)		
Median	18.5	16
Range	11-51	8-49
Anatomical site		
Femur		26
Tibia		8
Radius		3
Pelvis		2
Other		2
Clinical stage		
IIA		8
IIB/III		33

OS: osteosarcoma